CHAPTER-V

EMBEDDED DUMBBELL SHAPED DEEP EUTECTIC SOLVENT GEL META-STRUCTURE ABSORBER

5.1 Introduction

5.2 Design and optimization of dumbbell shaped DES gel MSA unit cell

5.3 Simulated absorption performance of dumbbell shaped DES gel MSA unit cell

5.4 Fabrication and absorption performance of dumbbell shaped DES gel MSA

5.5 Application study of the proposed MSA in antenna isolation

5.6 Chapter Summary

References

5.1 INTRODUCTION

Single square cuboid structured ionic DES gel MSAs studied in chapter IV, showed enhanced absorption bandwidth of more than 30% in comparison to similar single cuboid structure using slime, studied in chapter II. On conducting retractability studies on gel based cuboids, as carried out in chapter III, the DES gel is observed to slip off from matrix's edges as illustrated in Figure 5.1(a). This can be attributed to the poor affinity of silicone-rubber for ethylene glycol as demonstrated by wettability test, Figure 5.1(b). A structural modification in cuboidal DES gel resonator design is to be carried out to achieve a more stable embedded DES gel resonator structure, which can provide ease of restoration upon bending/stretching.

After investigating different structural geometry modifications, it is found that a gel bridge if introduced in between two adjacent DES gel cuboids restricts the slipping whilst keeping the advantage of cuboid geometry. The new structure because of its alikeness, is termed as dumbbell. The gel in the bridge cuboid gets stretched and provides a recoiling force (T) to oppose external force, F_{ext}, avoiding slipping, thus, assisting in keeping the gel in place, as schematized in Figure 5.1(c)(i) and (ii).

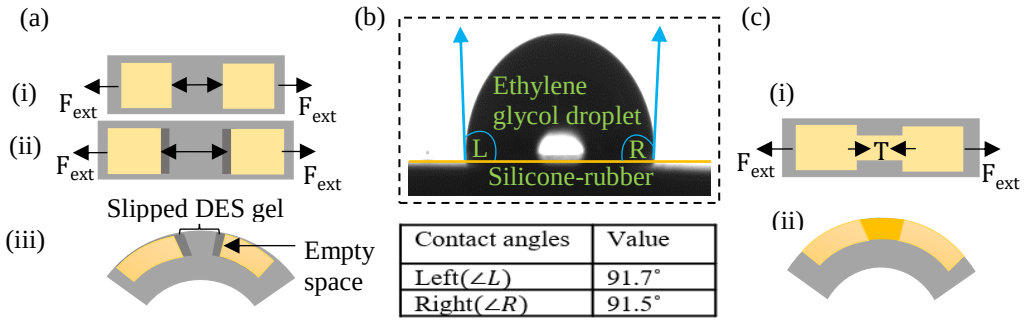

Figure 5.1 Schematic of (a) (i) DES gel MSA unit cell (top view), (ii) external force (F_{ext}) acting on MSA without cuboid bridge, (iii) bending and stretching of meta-structure (side view) without cuboid bridge. (b) Wettability test of silicone rubber with ethylene glycol and (c) stability of DES gel (i) and (ii) with cuboid bridge.

The dumbbell shaped DES gel MSA unit cell is designed, optimized and fabricated inhere. Absorption performance analysis is carried out. Studies of applicability of the MSA in enhancement of isolation in co-sited antennas is conducted.

5.2 DESIGN AND OPTIMIZATION OF DUMBBELL SHAPED DES GEL MSA UNIT CELL

The DES gel dumbbell structure is incorporated in silicone rubber substrate backed by copper tape. The enclosed DES gel structure is covered with a thin layer of silicone. Figure 5.2(a)-(c) shows the schematic of the proposed absorber.

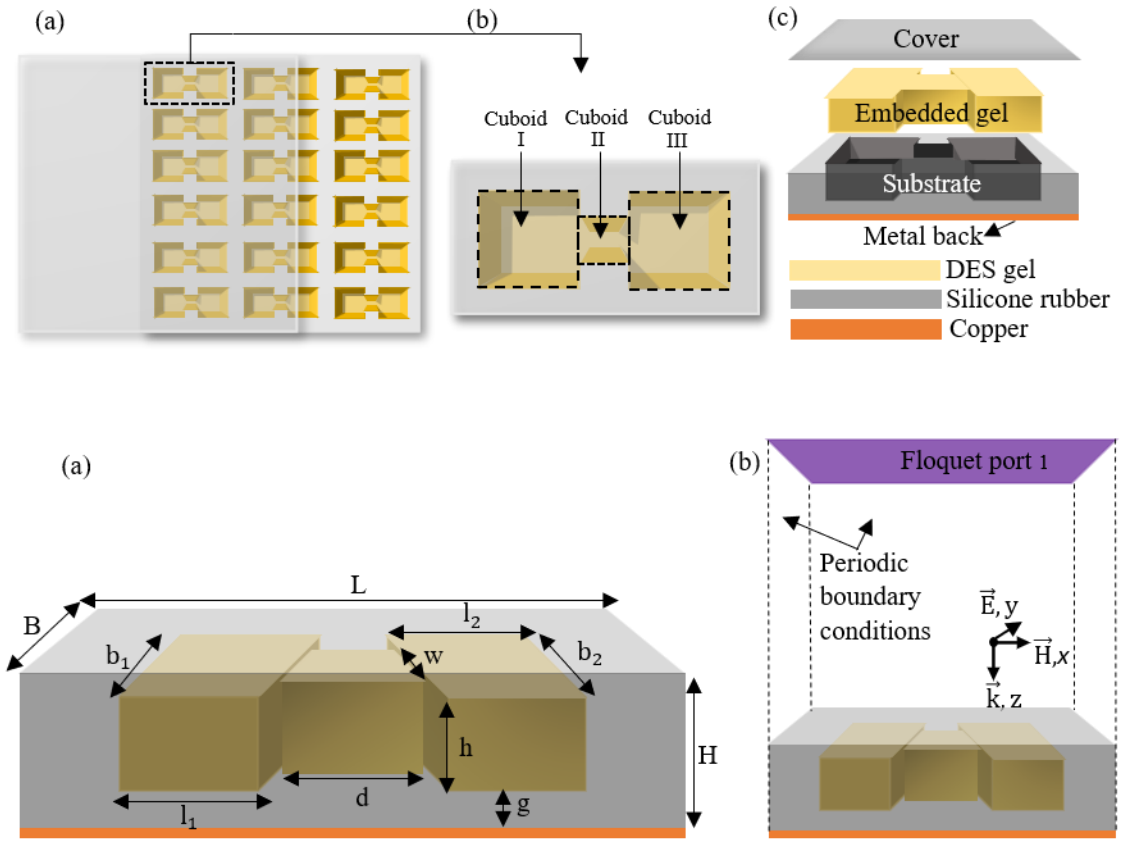

Figure 5.2 Schematic of (a) proposed MSA, (b) MSA unit cell top view and (c) components of the unit cell. (a) Dimensions of the MSA unit cell. (b) A complete simulation setup with periodic boundaries and Floquet port 1.

The dimensions of the unit cell as shown in Figure 5.2(a) are optimized using Floquet port in the far-field as shown in Figure 5.2(b) and the final optimized dimensions of the MSA unit cell are placed in Table 3. The optimization is carried out in - (I) thickness/height of both the silicone matrix and the gel to obtain absorption in X-band; (II) dimensions of both the cuboids I and III, of the dumbbell structure to obtain resonant frequency at around central frequency (~10.2 GHz), and (III) width of cuboid II to obtain a bandwidth >3 GHz. The dimensions of cuboid III are varied as ($l_2 \times b_2$)= 5 mm × 5 mm, 6 mm × 6 mm and 7mm × 7 mm. During optimization, it is found that when the dimensions of cuboids I and III are equal i.e., $l_1 = b_1 = l_2 = b_2 =$ 6mm, the reflection loss is minimum. Further when the size of cuboid II is (w × d) =

3 mm × 3 mm, the -10 dB absorption bandwidth enhances in the operating band. The silicone cover is kept at a thickness (~0.25 mm) to facilitate fabrication and to avoid the system becoming very bulky.

Table 5.1 Optimized parameter values of the designed meta-structure.

Parameter	Description	Magnitude (mm)
L	length of MSA unit cell	18
B	breadth of MSA unit cell	8.5
H	height of MSA unit cell	2.75
$\mathbf{l_1 = l_2}$	length of DES gel cuboids I and III	6
$\mathbf{b_1 = b_2}$	breadth of DES gel cuboid I and III	6
h	height of DES gel cuboids I, II and III	1.5
w	width of DES gel cuboid II	3
d	length of Des gel cuboid II	3
g	thickness of silicone below the dumbbell structure	1
	Top silicone cover thickness	0.25
	Copper tape thickness	0.035

5.3 SIMULATED ABSORPTION PERFORMANCE OF DUMBBELL SHAPED DES GEL MSA UNIT CELL

The simulated reflection loss (S_{11}) values of the MSA unit cell with dimensions of cuboid I as ($l_1 \times b_1$)= 6 mm × 6 mm and dimensions of cuboid III as ($l_2 \times b_2$)= 5 mm × 5 mm, 6 mm × 6 mm and 7mm × 7 mm are plotted in Figure 5.3 (a).

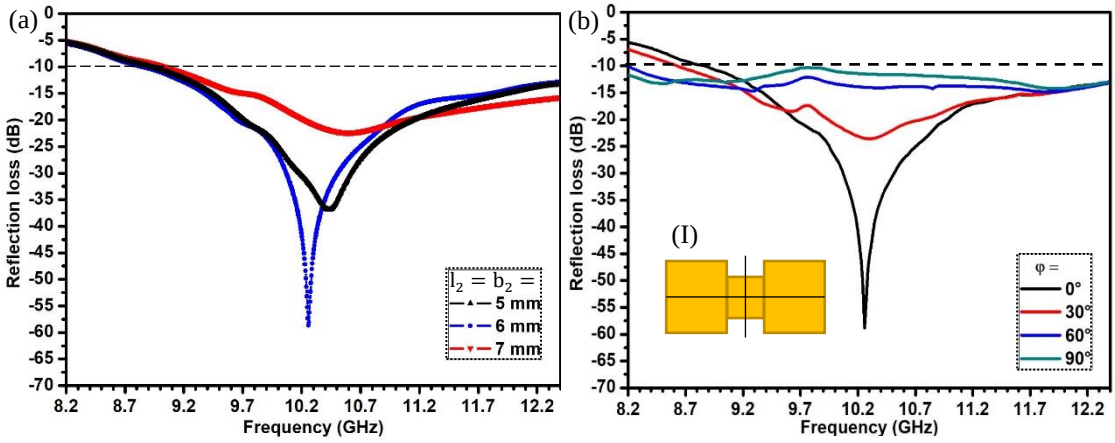

Figure 5.3 Reflection loss spectra of MSA for (a) different dimensions of cuboid III and (b) different polarization angles for a normally incident EM wave. Inset:(I) Schematic of two-fold symmetry in dumbbell structure.

The MSA with cuboids of ($l_i \times b_i$)= 6 mm × 6 mm shows a reflection loss of about – 59 dB centred at around 10.26 GHz with a -10 dB bandwidth of 3.6 GHz covering almost 80% of the X-band.

The effect of various polarization angles on the reflection loss spectra of the MSA is studied, Figure 5.3(b), and the designed MSA is found to behave differently at different polarization angles due to the two-fold symmetry of the dumbbell structure, Figure 5.3(b)-inset(I), nevertheless, -10 dB bandwidth is maintained upto $\pm 90°$.

The reflection loss spectra of the MSA is studied for various oblique incidence under both transverse electric (TE) and transverse magnetic (TM) modes. Figure 5.4 shows that the reflection loss spectra of the MSA are dependent on the incident angles of EM wave. (Figure 5.4(a) and (b)). The insensitivity is limited up to $\pm 40^{\circ}$ for -10 dB absorption which covers more than 80% of the X-band.

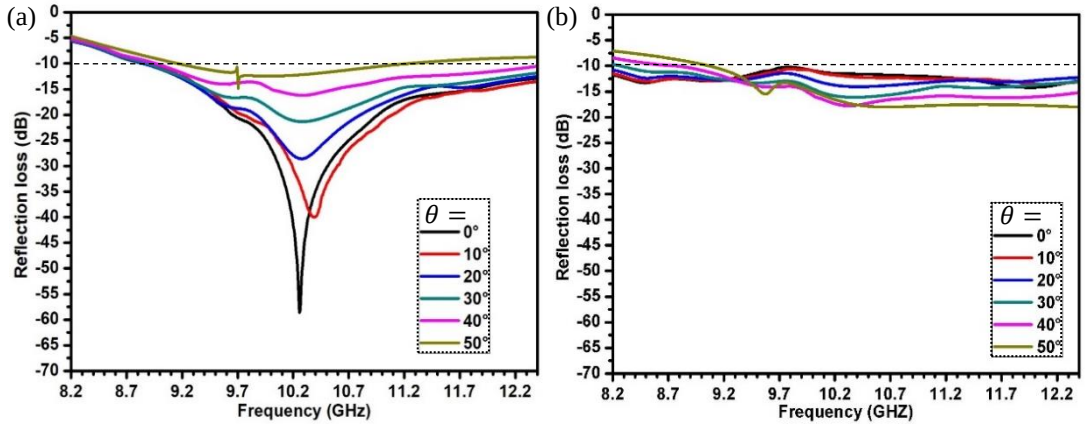

Figure 5.4 (a) Reflection loss spectra at different incident angles for (a) TE mode and (b) TM mode.

The normalized impedance for the absorber with cuboids of $(l_i \times b_i)$= 6 mm × 6mm is plotted in Figure 5.5(a). At the resonating frequency, it is found that both the complex quantities are negative ($\varepsilon_a = -0.2 + 16.9$ and $\mu_a = -0.25 + 16.9$), Figure 5.5(b)-(c) using equations (4.3) and (4.4). Thus, confirming the structure to exhibit properties of a metamaterial [1].

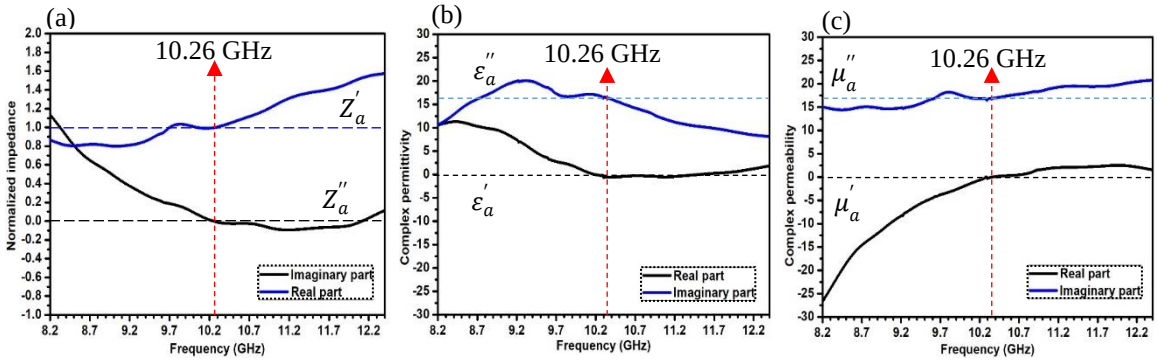

Figure 5.5 Simulated (a) reflection loss spectra of MSA for different dimensions of cuboid III and (b) normalized impedance of the MSA with $(l_i \times b_i) = 6$ mm × 6 mm.

The reflection loss of the MSA unit cell is simulated for different bending curvatures. - 10 dB bandwidth remains same for curvature radius up to 20 mm when bent along the breadth of the MSA. There is a minimal shift in the resonant frequency and reflection loss increases with increasing curvature, Figure 5.6. This may be attributed to the decrease of effective area of the absorber facing the normal incident em wave. On further bending, reflection loss deteriorates drastically.

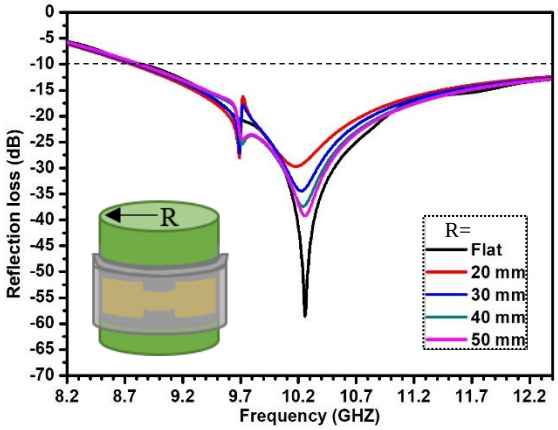

Figure 5.6 Simulated reflection loss spectra at different bending radii of the MSA unit cell, inset: representation of bending radius (R).

The interaction of the designed MSA with microwave is found to resemble similar mechanism as the DES-gel-Si-MSA studied in chapter IV. At resonant frequency (10.26 GHz), the electric field distribution in Figure 5.7(a) can be seen to be concentrated at the edges of the DES gel cuboids I and III. On the other hand, the magnetic field component is concentrated within the DES gel dumbbell structure Figure 5.7(c). The induce current is depicted in Figure 5.7(d). The induced current

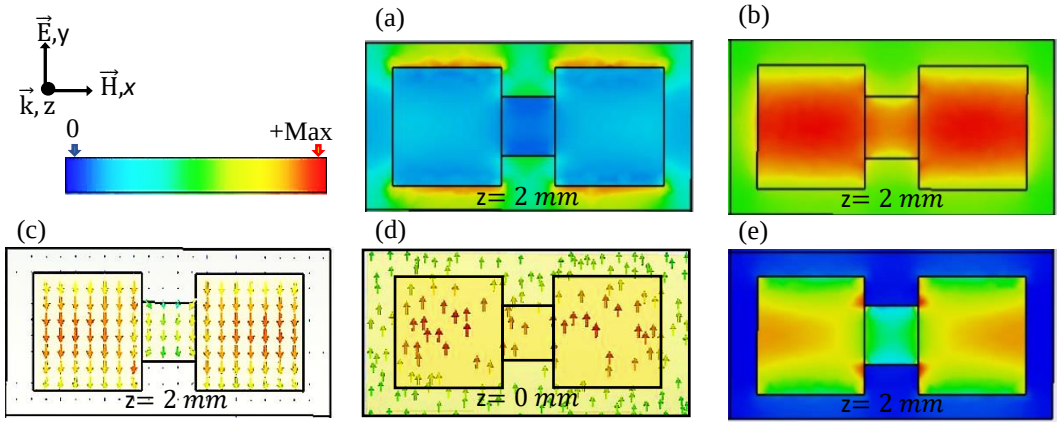

Figure 5.7 Simulated (a) E-field density (b) H-field density, (c) induced current density, (d) Surface current on the ground plane and (e) power loss density of MSA, at 10.26 GHz.

density, Figure 5.7(c) goes 180˚ out of phase with the surface current, Figure 5.7(d), on the ground, reducing the reflection loss at the resonant frequency.

Figure 5.7(e) shows the power loss distribution in the MSA unit cell. With a simulation power of 0.5 W, the values of scattered power in individual material within the MSA unit cell at X-band have been plotted in Figure 5.8. The power loss in the DES gel is ~0.47 W while in copper ~0 W. In the silicone rubber matrix, the power loss is ~0.1 W. The maximum power loss takes place in the DES gel structure.

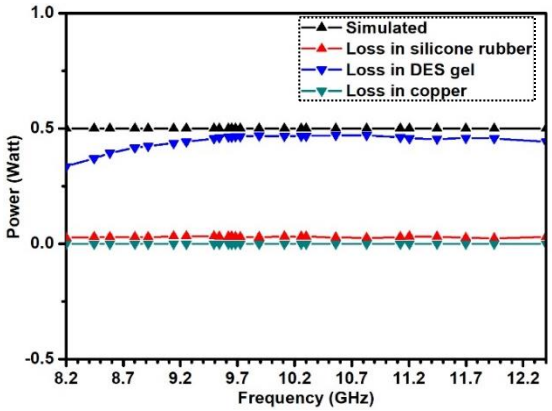

Figure 5.8 Simulated power loss in each material of the MSA unit cell.

5.4 FABRICATION AND ABSORPTION PERFORMANCE MEASUREMENT OF DUMBBELL SHAPED DES GEL MSA

MSA unit cell is developed using the optimized dimensions from Table 5.1. The developed absorber is shown in the image in Figure 5.9.

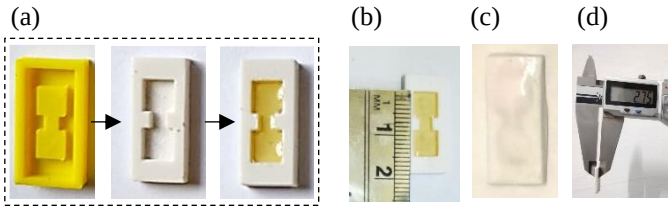

Figure 5.9 (a) Development of MSA sample. Developed absorber (b) uncovered and (c) covered. (d) Thickness of the MSA.

The developed absorber is tested for its tensile strength and the values are plotted in Figure 5.10(a). A maximum elongation at break is found to be ~140%. A comparison plot for experimental and simulated reflection loss curves is presented in Figure 5.10(b). Reflection loss is observed to be -40.02 dB at 10.55 GHz with a -10 dB

bandwidth of ~ 3 GHz. It is observed that the experimental results are in close proximity to the simulated results. Cuboid III with the dimensions $l_2 \times b_2 =$ 5 mm × 5 mm and 7 mm × 7 mm are fabricated alongwith (Figure 5.10(c)-inset) and their reflection loss is measured. Figure 5.10(c) plots the measured reflection loss, the trend is similar to one observed in simulated results Figure 5.3(a). The shift in resonant frequency with varying dimensions indicates the structural tunability of the absorber that MMAs claimed to have [2, 3]. Performance results are tabulated in Table 5.2.

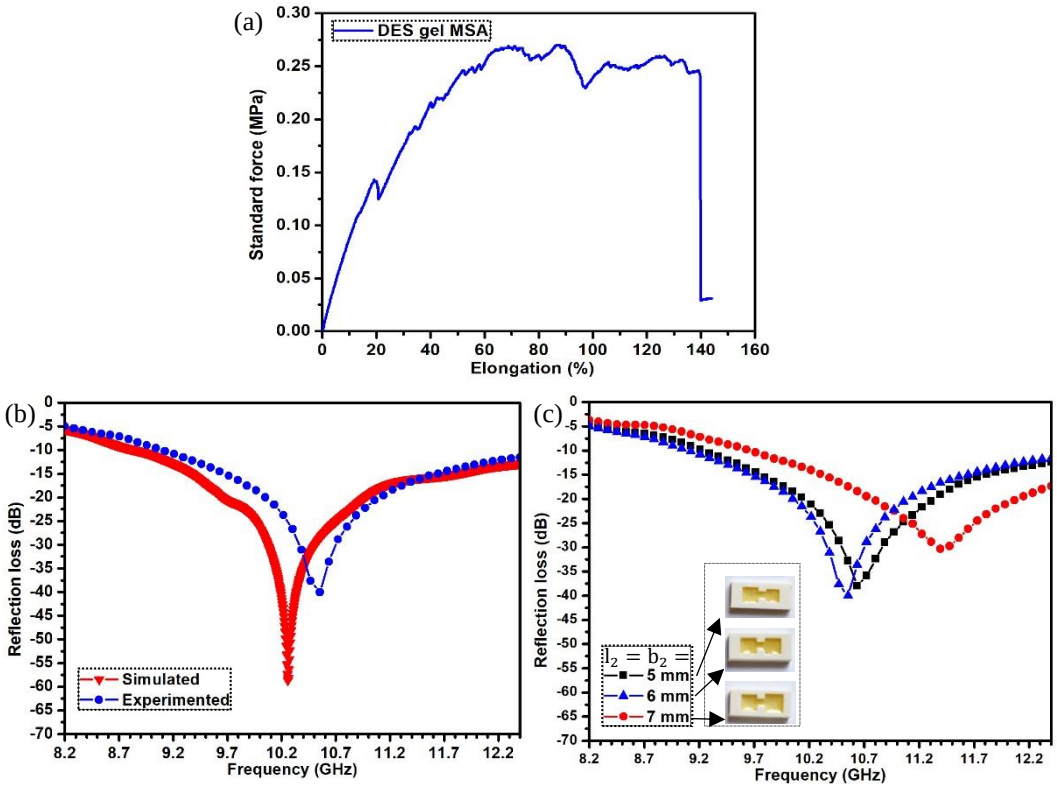

Figure 5.10 (a) Tensile strength of dumbbell shaped DES gel MSA. Experimental and simulated reflection loss curves of (b) MSA ($l_1 = b_1 = l_2 = b_2 = 6$ mm). (c)Experimental MSA with $l_1 = b_1 =$ 6 m and $l_2 = b_2$= 5 mm, 6mm and 7 mm, inset: fabricated MSAs.

Table 5.2 Simulation vs. experimental results for cuboid I dimension 6 mm × 6 mm and varying cuboid III dimension.

	MSA with cuboid III of $l_2 = b_2$ (mm)	**RF (GHz)**	**RL (dB)**	**-10 dB BW (GHz)**	**% coverage of X-band**
Simulated	5	10.43	-36.92	3.48	82.9
	6	10.26	-59.10	3.55	84.5
	7	11.11	-26.26	3.36	80.0
Experimental	5	10.64	-37.95	3.15	75.0
	6	10.55	-40.02	3.34	79.5
	7	11.39	-30.30	2.69	64.0

5.5 APPLICATION STUDY OF THE PROPOSED MSA IN ANTENNA ISOLATION

The shrinking communication technology has placed antennas closed together in a single platform. The electromagnetic fields from one antenna bleed over undesirably into another antenna. This coupling deteriorates the performance of the system and corrupts trans-received information. Figure 5.11(a), represents a co-sited antenna system transmitter (Tx) and receiver (Rx) leading to EMI. Antenna isolation measures the extent to which the coupling and leakages as sidelobes/back lobes can be reduced [4]. EMI suppression between co-sited antennas will enhance antenna isolation.

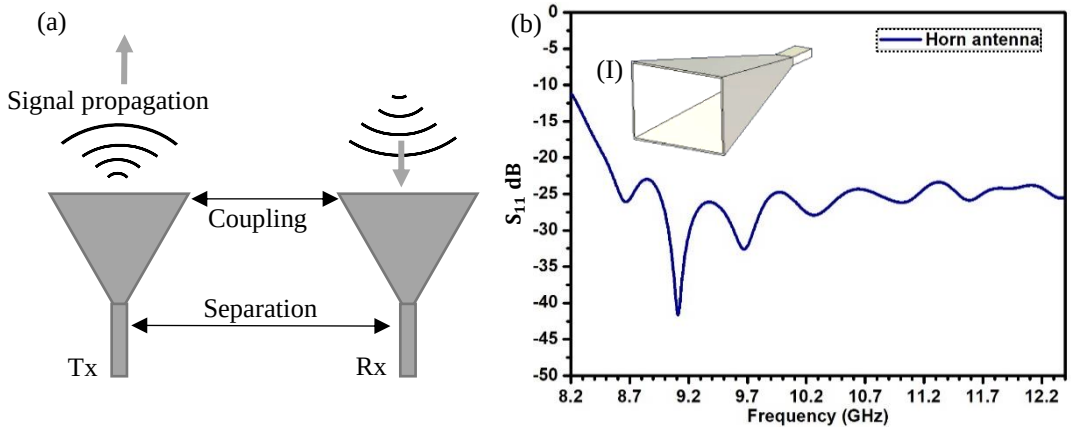

Figure 5.11 (a) Schematic of two co-sited horn antennas. (b) S_{11} curve for designed horn antenna, inset: (I) schematic of the antenna.

Here, simulation results of EMI suppression and hence improved antenna isolation is presented using the developed DES gel MSA. The simulation is carried out in three steps- (I) Two identical broadband horn antennas, Tx and Rx, with $S_{11} \geq -20$ dB and far-field ≥ 1.5 m at X-band are designed. The performance of the designed antenna over the X-band is shown in Figure 5.11(b) with a schematic of the antenna in Figure 5.11(b)-inset:(I). (II) Transmission (S_{21}) from Tx to Rx is measured at two different near field distances, x=15 cm and 30 cm, Figure 5.12, by inserting different materials including MSA, between E-plane apertures of the horn antennas such that the materials have a good contact with the outer metal part of Tx and Rx, Figures 5.13(a) and (b). Each material is so chosen which may in one way or other interact with co-sited antennas performance.

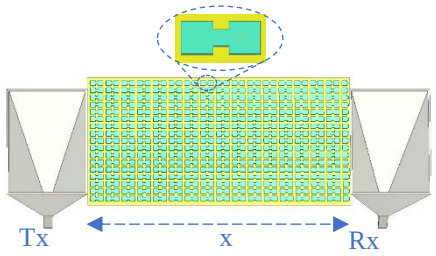

Figure 5.12 Illustration of placement of MSA between the X-band horn antennas with separation distance x.

At first, the simulations are carried out with lossy materials with different permittivity and loss tangent values which could potentially be found in between co-sited antennas viz., (i) vacuum ($\varepsilon_a' = 1$, $\frac{\varepsilon_a''}{\varepsilon_a'} \sim 0$); (ii) FR4 ($\varepsilon_a' = 4.3$, $\frac{\varepsilon_a''}{\varepsilon_a'} \sim 0.025$) and (iii) air ($\varepsilon_a' = 1.00059, \frac{\varepsilon_a''}{\varepsilon_a'} \sim 0$). Next, the simulations are conducted with the constituent materials of the dumbbell shaped DES gel MSA i.e., (i) silicone rubber, (ii) DES gel and (iii) copper placed in between the antennas. As FR4, copper is frequently used in integrated electronic circuits and systems apart from being a component of the absorber. The dimension of all the simulated materials are kept same as the absorber.

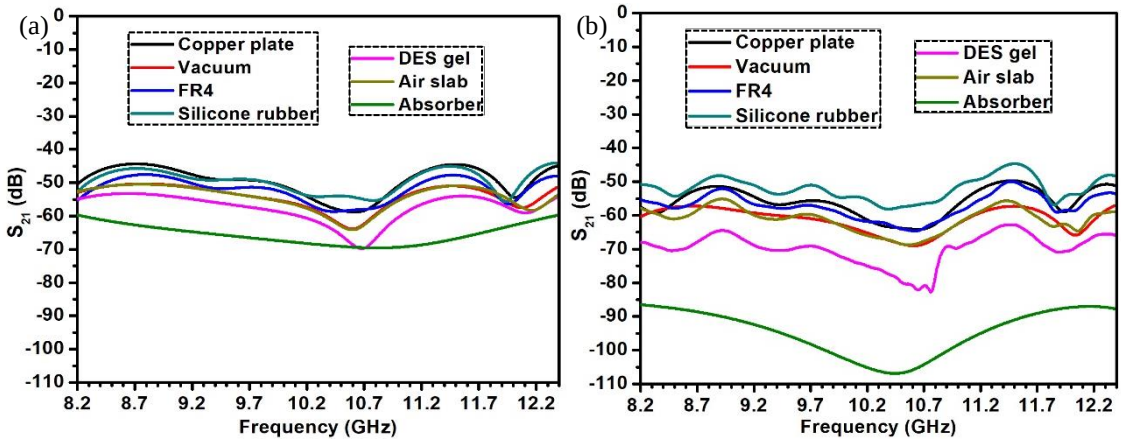

Figure 5.13 S_{21} curves with different materials placed between horn antennas (a) 15 cm and (b) 30 cm apart respectively.

It is observed that in both of the simulated separations, the designed dumbell shaped DES gel MSA offers the highest resistance to the transmission of EM waves from Tx to Rx among all the materials.

(III) The isolation is determined by taking the difference between the S_{21} values of the reference and the absorber (S_{21}(reference) – S_{21}(absorber)) [5]. The isolation improvement in horn antennas with reference copper plate for the two separations, x=15 cm and 30 cm are shown in Figure 5.14(a) and air for the two separations, x=15 cm and 30 cm are shown in Figure 5.14(b). The results are placed in Table 5.3.

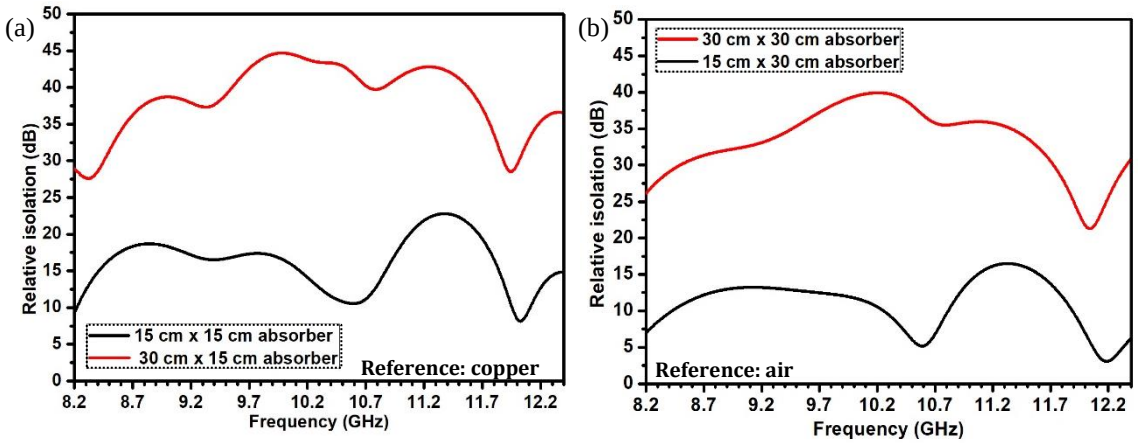

Figure 5.14 Relative isolation curves with MSA placed between horn antennas with respect to (a) copper and (b) air.

Table 5.3 Results of relative isolation.

Reference material	Separation x (cm)	Average isolation (dB)	Peak isolation value (dB)	Frequency at peak isolation (GHz)
Copper plate	15	16.1	22.8	11.3
	30	38.6	44.5	9.9
Air slab	15	11.13	16.5	11.34
	30	33.4	39.94	10.22

To have a better understanding of the isolation improvement in the antennas, electric energy density is investigated at 9.9 GHz at x=30 cm. Electric energy density is studied as in the proposed MSA dielectric loss dominates. Normalized electric density in dB for the co-sited horn antenna system with the reference air as well as copper plate Figure 5.15(a) and (b) and the DES gel MSA, Figure 5.15(c) in between is computed. It is observed that the normalized electric energy density in the Rx drops down to -80 dB with the use of the MSA.

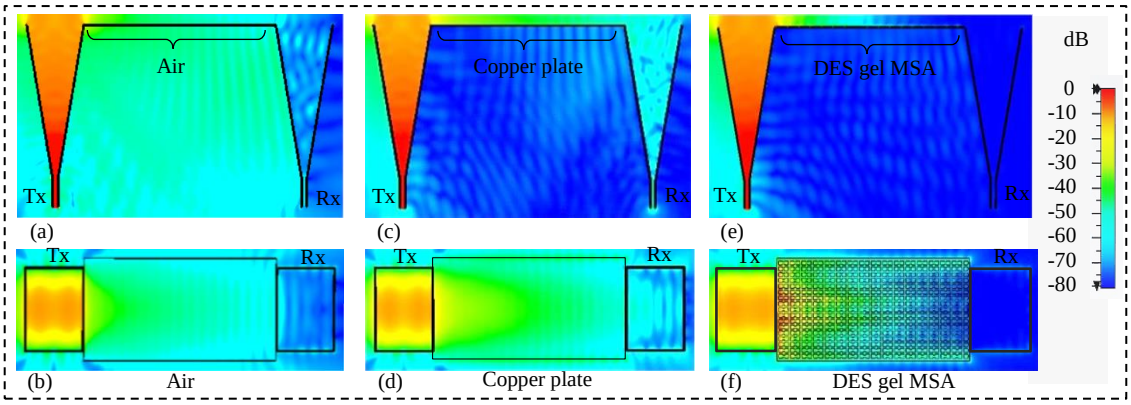

Figure 5.15 The electric energy density simulation for co-sited horn antennas at 9.9 GHz with air reference (a) side view, (b) top view, copper reference (c) side view, (d) top view and DES gel MSA (e) side view and (f) top view, placed in between them.

5.6 CHAPTER SUMMARY

An X-band meta-structure absorber is developed embedding DES gel in silicone matrix. The periodic structures are shaped as dumbbells which provide stability to the structure. The developed MSA shows a wide bandwidth absorption at wide polarization and incident angles. One of the applications of the proposed absorber in improving antenna isolation is demonstrated with the simulation results. It is found that the isolation improves by more than 30 dB when placed between two X-band horn antennas. The specifications of the dumbbell shaped DES gel MSA are illustrated in Table 5.4.

Table 5.4 Specifications of the dumbbell shaped DES gel MSA.

Result→	***Measured***								***Simulated***	
Parameter	**RF (GHz)**	**RL (dB)**	**% coverage of X-band**	**10 dB RCSR BW (GHz)**	**Thickness**	**WA (%)**	**ρ (g cm^{-3})**	**P: L & B (mm)**	**PA-T**	**IA-T**
Values	10.6	-40.02	~80	9.06-12	2.75 ($0.0775\lambda_0$)	0.6	~1.27	18 × 8.5	±90°	±40°
Note: RF- Resonant frequency, RL-reflection loss, BW- bandwidth λ_0-lowest operating frequency, WA-water absorbance, **ρ**- density, P-periods: L- length and B- breadth of MSA unit cell, PA-T- polarization angle tolerance, *IA-T-incidence angle tolerance*.										

REFERENCES

[1] Veselago, V.G., Electrodynamics of substances with simultaneously negative and*. Usp. fiz. nauk*, 92(7): 517-526, 1967.

[2] Lapine, M., et al., Structural tunability in metamaterials*. Applied Physics Letters*, 95(8): 084105, 2009.

[3] Lapine, M. and S. Tretyakov, Contemporary notes on metamaterials*. IET microwaves, antennas propagation,* 1(1): 3-11, 2007.

[4] Victor, O., N.G. GN, and D. Onyishi, *Antenna Isolation Technique for Interference Reduction in a Co-Site System*, in *International Journal of Advanced Research*. 2013.

[5] Hamid, S. and D. Heberling. *Experimental Demonstration of Antenna Isolation Improvement using Planar Resonant Absorbers*. In *2019 International Symposium on Electromagnetic Compatibility-EMC EUROPE*, 2019 pages 351-354, 2019, IEEE.